Indian Journal of Pure & Applied Physics
Vol. 56, December 2018, pp. 965-969

# Effect of Ni ion irradiation on microstructure and corrosion properties of $Zr_{59}Nb_3Cu_{20}Al_{10}Ni_8$ amorphous alloy

Poonam Sharma[a,b], Anil Dhawan[b]*, S Faheem Naqvi[b] & S K Sharma[a]

[a]Department of Physics, Malaviya National Institute of Technology, Jaipur 302 017, India

[b]Department of Physics, Anand International College of Engineering, Jaipur 303 012, India

*Received 12 January 2018; accepted 15 May 2018*

The amorphous $Zr_{59}Nb_3Cu_{20}Al_{10}Ni_8$ alloy has been irradiated by 100 MeV $Ni^{+7}$ ion beam at the fluence rates of $1\times10^{13}$ and $1\times10^{14}$ ions/cm$^2$ at room and elevated temperature. The effect of irradiation on structure sensitive properties of Zr-based amorphous alloys has been investigated in this study using XRD and FESEM and potentiodynamic polarization study. The results reveals that there are no significant changes in the microstructure at lower fluence rate but the formation of nanocrystalline structures have been observed at the higher fluence rates and the results have been corroborated using corrosion studies.

**Keywords:** Irradiation, X-ray diffraction, FESEM, Potentiodynamic polarization, Corrosion

## 1 Introduction

The bulk metallic glasses are interesting materials due to their unique properties, such as superior strength and hardness, excellent corrosion resistance[1-3]. Metallic glasses share the properties of both the metals as well as glasses and exhibit superior mechanical and chemical properties[4]. The ion irradiation introduces certain changes in these properties and induces phase transition. In the case of amorphous alloys certain phases can be produced within the amorphous matrix by ion irradiation that can enhance the surface properties. Carter *et al.*[5] have reported that Cu ion irradiation induce the nano-crystalline formation in $Zr_{55}Cu_{30}Al_{10}Ni_5$ bulk amorphous alloy. Iqbal *et al.*[6] have studied ion irradiation with $Ar^+$ ions on $Zr_{55}Cu_{30}Al_{10}Ni_5$ bulk amorphous alloy and noticed improvement in mechanical properties of the irradiated areas of the alloy. In one of the study on $Zr_{41.2}Ti_{13.8}Cu_{12.5}Ni_{10}Be_{22.5}$ metallic glass irradiated with Ni ion beam of high energy shows an enhancement in ductility by promoting shear band intersection, which shows that irradiation can enhance overall mechanical properties of amorphous alloys[7]. Few more studies including amorphous $Ti_{60}Ni_{40}$ alloy irradiated with $Ni^{+11}$ ions exhibits superior corrosion resistance in 1M $HNO_3$ than virgin amorphous specimen[8]. In another study related to mechanical properties such as hardness and Young Modulus both were found decreased in $Zr_{52.5}Cu_{17.9}Ni_{14.6}Al_{10}Ti_5$ alloy irradiated with 3 Mev $Ni^+$ ions at room temperature, whereas no significant changes were observed[9] at 200 °C. Menéndez *et al.*[10] have also studied the structural, mechanical and corrosion behaviour of Ar ion irradiated $Zr_{55}Cu_{28}Al_{10}Ni_7$ and $Ti_{40}Zr_{10}Cu_{38}Pd_{12}$ alloys at room and elevated temperature. It has been reported that nano-crystalline structures were formed due to irradiation and these alloys exhibit improvement in mechanical and corrosion resistance at elevated temperature.

In the present study, the effect of high energy $Ni^{+7}$ ion irradiation on the structure sensitive properties of $Zr_{59}Nb_3Cu_{20}Al_{10}Ni_8$ amorphous alloys at room and elevated temperature was examined. Microstructure, surface morphology and corrosion behaviour of these ion irradiated samples were investigated.

## 2 Experimental

### 2.1 Materials and phase identification

The as-received $Zr_{59}Cu_{20}Ni_8Al_{10}Nb_3$ ribbon samples of dimension (1.0 cm×0.3 cm×30 μm) were investigated in the present study. Samples were cleaned with acetone and distilled water and dried in air. Phase analysis of the ribbon sample was carried out by X-ray diffraction (XRD) technique with XPERT PRO X-ray diffractometer using CuKα radiations.

### 2.2 Ion irradiation

The specimens of suitable size (1 cm×0.3 cm× 30 μm) were cut from the melt spun ribbons of

*Corresponding author (E-mail: dr.anildhawan11@gmail.com)

amorphous $Zr_{59}Cu_{20}Ni_8Al_{10}Nb_3$ alloy. Specimens were cleaned with ethanol prior to the experiment. For irradiation, the samples were stuck to the ladder with the help of sample holder. The samples were irradiated with $Ni^{+7}$ ion beam of 100 MeV energy at different fluence rate of $1\times10^{13}$ and $1\times10^{14}$ ions/cm$^2$ at room and elevated temperature, i.e., 200 °C. The experiment was carried out at Inter University Accelerator Centre (IUAC), New Delhi. The vacuum of irradiation chamber was maintained below $10^{-7}$ torr during the experiment. The beam current was kept between 0.8 to 1 pnA (particle nano ampere) on the samples during the irradiation to minimize the ion beam heating.

#### 2.3 Microstructural characterization and surface morphology

The $Ni^{+7}$ ion implanted ribbon samples were characterized by X-ray diffraction (XRD). XRD pattern was acquired on an XPERT PRO X-ray diffractometer using CuKα radiation. Surface morphology of the as-spun and $Ni^{+7}$ ion irradiated samples at room and elevated temperature at $1\times10^{14}$ ions/cm$^2$ doses were examined by FESEM using Nano-FESEM system at MRC, MNIT, Jaipur.

#### 2.4 Electrochemical measurements

The electrochemical behaviour of as cast and $Ni^{+7}$ ion implanted $Zr_{59}Cu_{20}Ni_8Al_{10}Nb_3$ alloy at $1\times10^{14}$ ions/cm$^2$ dose at room and elevated temperature in 1M $HNO_3$ medium was investigated using a potentiostat (Autolab-AUT84276) consisting of a three-cell electrode. Samples were cleaned with ethanol and distilled water and dried in air before the experiment. These glassy samples were used as working electrodes; Ag/AgCl (3 M KCl) and platinum foil were used as reference and counter electrodes, respectively. An area of 1.0 cm×0.3 cm of the sample was exposed and the open circuit potential (OCP) was monitored for 20 min. Potentiodynamic polarization tests were performed at the scanning rate of 0.001 V/s from -0.2 V below OCP to 2.1 V. The values of corrosion potential ($E_{corr}$) and corrosion current density ($I_{corr}$) were obtained by Tafel method. The electrochemical experiments were repeated for checking the reproducibility of the results.

## 3 Results and Discussion

#### 3.1 Microstructural characterization

Figure 1 shows the XRD pattern of as spun $Zr_{59}Nb_3Cu_{20}Al_{10}Ni_8$ ribbon sample, which exhibits the presence of a broad halo peak, indicating the amorphous nature of the alloy. Figure 2 is a XRD pattern of $Ni^{+7}$ ion irradiated $Zr_{59}Nb_3Cu_{20}Al_{10}Ni_8$ ribbon sample with doses of $1\times10^{13}$ and $1\times10^{14}$ ions/cm$^2$ at room and elevated temperature, i.e., 200 °C. It showed that no significant changes have been observed in the microstructure of glassy alloy at lower fluence rate, whereas at higher fluence rate, comparatively sharp peak was observed which is possibly due to formation of nanocrystalline structure.

In high energy ion irradiation process, the target atoms of metallic glasses are displaced from their initial sites, which may create vacancy-like defects. It increases the free volume within the system and

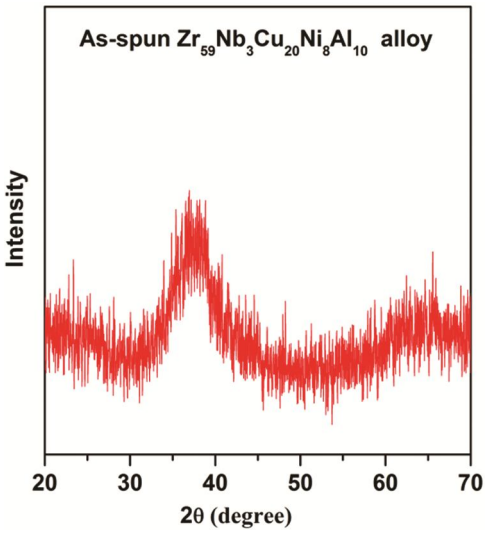


Fig. 1 – XRD pattern of as spun $Zr_{59}Nb_3Cu_{20}Al_{10}Ni_8$ glassy ribbon.

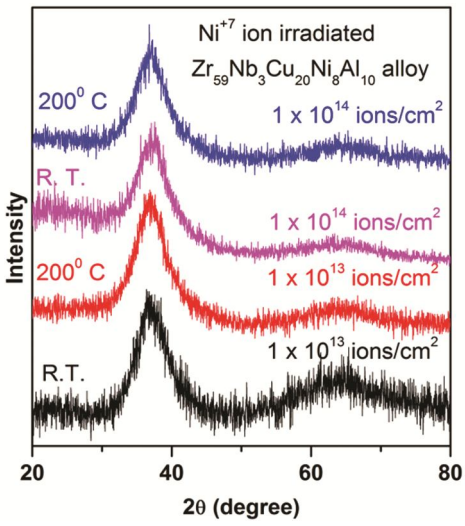


Fig. 2 – XRD pattern of $Ni^{+7}$ ion irradiated $Zr_{59}Nb_3Cu_{20}Al_{10}Ni_8$ glassy ribbon at $1\times10^{13}$and $1\times10^{14}$ ions/cm$^2$ doses at room and elevated temperature.

enhances the atomic mobility. The enhanced atomic mobility will lead to a increased short-range order and the subsequent nucleation resulting into the formation of nanocrystalline structure[11,12]. In another study, Carter *et al.*[5] have also reported the formation of nanocrystalline phases in $Zr_{55}Cu_{30}Al_{10}Ni_5$ metallic glass after irradiation with 1 MeV Cu ions at a fluence rate of $1\times10^{16}$ ions/cm$^2$. Furthermore, in a recent study it has been reported that ion bombardment induces structural relaxation through the atomic diffusion process which initiates the crystallization[13]. In the present research work, the XRD pattern (Fig. 2) exhibits that the lower fluence rate does not changes the structure of amorphous alloy whereas, higher fluence rate significantly alter the structural properties. These structural changes are attributed to the knock-on effect caused by compressive stress originated from larger momentum, which is produced from the bombardment of a large number of ions on the sample[14]. Since, ion beam irradiation causes rise in the temperature of the sample but this rise in temperature is controlled by maintaining the low beam current 0.8-1.0 pnA.

### 3.2 Surface morphology

Figure 3 (a-e) shows the FE-SEM micrographs of as spun and irradiated $Zr_{59}Nb_3Cu_{20}Al_{10}Ni_8$ glassy ribbon at $1\times10^{14}$ ions/cm$^2$ fluence rate at room and elevated temperature (200 °C). Figure 3(a) revealed that the surface of as-spun glassy ribbon was smooth

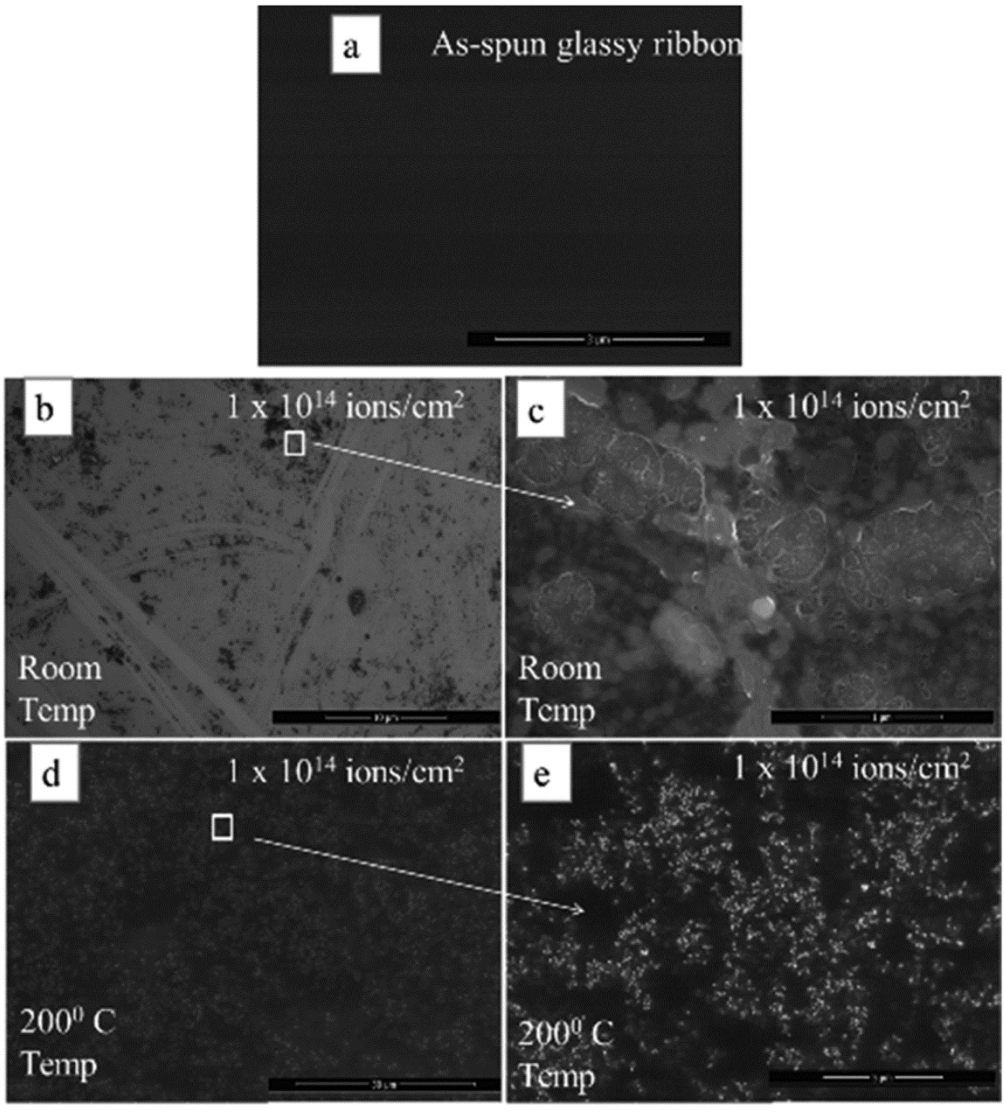


Fig. 3 – FESEM micrographs of (a) as spun and $Ni^{+7}$ ion irradiated $Zr_{59}Nb_3Cu_{20}Al_{10}Ni_8$ glassy ribbon at $1\times10^{14}$ ions/cm$^2$ dose, (b) at room temperature, (c) higher magnification image of marked area in Fig. 3 (b), (d) at elevated temperature and (e) higher magnification image of marked area in Fig. 3 (d).

and clean. Irradiation affected area can be seen on the surface of irradiated $Zr_{59}Nb_3Cu_{20}Al_{10}Ni_8$ glassy ribbon at $1\times10^{14}$ ions/cm$^2$ fluence rate at room temperature (Fig. 3(b)). High magnification image of marked area is shown in Fig. 3(c), which indicates the initiation of nano-crystal formation. Figure 3(d) is a micrograph of $Ni^{+7}$ ion irradiated surface of $Zr_{59}Nb_3Cu_{20}Al_{10}Ni_8$ glassy ribbon at $1\times10^{14}$ ions/cm$^2$ fluence rate at elevated temperature and it is found that at elevated temperature, micrographs exhibit the formation of nano-crystal structures which were clearly visible in high magnification image (Fig. 3(e)).

### 3.3 Potentiodynamic polarization study

Figure 4 shows the polarization curves, measured on the as-spun and $Ni^{+7}$ ion irradiated $Zr_{59}Nb_3Cu_{20}Al_{10}Ni_8$ glassy ribbon at $1\times10^{14}$ ions/cm$^2$ dose at room and elevated temperature in 1 M $HNO_3$ medium. Corrosion parameters such as $E_{corr}$ and corrosion current density $I_{corr}$ were calculated and summarized in Table 1. The $I_{corr}$ values were estimated by applying the Tafel slope method[15]. As shown in Fig. 4, as spun $Zr_{59}Nb_3Cu_{20}Al_{10}Ni_8$ glassy ribbons shows clear passivity in nitric acid medium with a broad passive region. Irradiated alloys also follow the similar trend in nitric acid medium. The irradiated alloy at $1\times10^{14}$ ions/cm$^2$ dose shows minor decrease in value of corrosion potential ($E_{corr}$) and minor increase in value of corrosion current density ($I_{corr}$) than that of as spun alloy (Table 1). The $E_{corr}$ value of irradiated alloy at elevated temperature has insignificantly increased and $I_{corr}$ value has slightly decreased. A significant difference could not be observed in potentiodynamic polarization curve of irradiated sample. But it can be revealed from Fig. 4 that the corrosion resistance has not been improved after irradiation at room as well as elevated temperature which is attributed to the formation of nano crystalline structure.

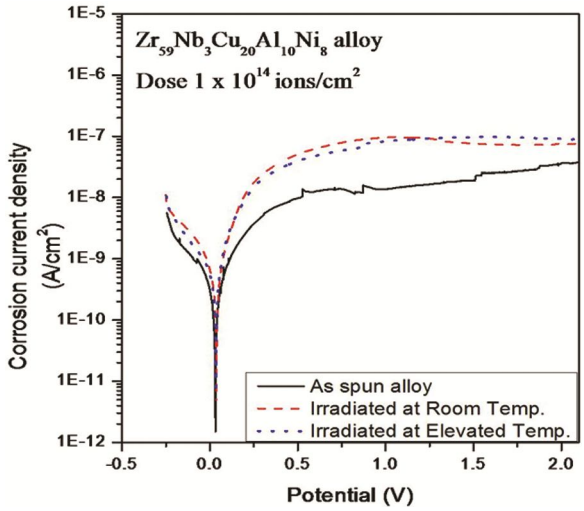


Fig. 4 – Potentiodynamic polarization curve of as spun and 100 MeV $Ni^{+7}$ ion irradiated $Zr_{59}Nb_3Cu_{20}Al_{10}Ni_8$ glassy alloy at $1\times10^{14}$ ions/cm$^2$ dose at room and elevated temperature (200 °C) in 1 M $HNO_3$.

Table 1 – Polarization parameter for as cast and $Ni^{+7}$ ion implanted $Zr_{59}Cu_{20}Ni_8Al_{10}Nb_3$ alloy at $1\times10^{14}$ ions/cm$^2$ dose at room and elevated temperature in 1M $HNO_3$ medium.

| Sample | $E_{corr}$ (V) | $I_{corr}$ (A/cm$^2$) |
|---|---|---|
| As spun alloy | 0.0316 | $4.391\times10^{-10}$ |
| Irradiated at room temp. ($1\times10^{14}$ ions/cm$^2$ dose) | 0.0286 | $6.302\times10^{-10}$ |
| Irradiated at elevated temp. ($1\times10^{14}$ ions/cm$^2$ dose) | 0.0293 | $4.539\times10^{-10}$ |

Perez-Bergquist *et al.*[9] has studied microstructural and mechanical properties of a $Zr_{52.5}Cu_{17.9}Ni_{14.6}Al_{10}Ti_5$ bulk metallic glass irradiated with 3 MeV Ni ions at room temperature and elevated temperature (200 °C) and no significant micro structural changes were observed in TEM investigations of irradiated sample. In present study 100 MeV $Ni^{+7}$ ion beam has been used in irradiation process so surface changes have been obtained in microstructure of Zr-based bulk amorphous alloy. It is well known that partial crystalline phases have deleterious effect on corrosion resistance[16]. All the potentiodynamic polarization curves of as spun and irradiated alloys shows a passivation plateau which shows the formation of passive film on the surface of alloy in nitric acid environment. Also, the presence of Nb element promotes an improvement in the corrosion resistance due to formation of niobium oxide film[17]. Thus, Ni ion irradiation could not improve the corrosion resistance of Zr-based bulk amorphous alloy at room and elevated temperatures.

## 4 Conclusions

The effect of 100 MeV $Ni^{+7}$ ion irradiation on $Zr_{59}Nb_3Cu_{20}Al_{10}Ni_8$ glassy ribbon at $1\times10^{13}$ and $1\times10^{14}$ ions/cm$^2$ fluence rate was studied at room and elevated temperatures. XRD results revealed that the amorphous nature of glassy ribbon has not been changed after $Ni^{+7}$ ion irradiation at low fluence rate. Though, nano-crystalline phases were observed for the glassy ribbon at higher fluence rate. FE-SEM micrographs have also revealed the formation of nano-crystalline structures on the surface of irradiated samples at higher fluence rate. These nano-crystalline structures are not improving the overall corrosion

resistance of the alloy and due to which the as-spun glassy ribbon showed better corrosion resistance in nitric acid medium as compared to the irradiated samples.

**Acknowledgement**

The financial support for this work under BRNS/DAE Research project No. 2011/36/44-BRNS/1974 is gratefully acknowledged. Thanks are due to Dr U Kamachi. Mudali, IGCAR, Kalpakkam for providing the specimens. We are also thankful to IUAC, Delhi for allocating beam time for high energy irradiation studies and Dr Pawan Kumar Kulriya for his guidance and support throughout irradiation studies. We are also beholden to Dr R K Duchaniya for corrosion testing and MRC, MNIT Jaipur for XRD and FESEM facility.

**References**

1 Wang W H, Dong C & Shek C H, *Mater Sci Eng R*, 44 (2004) 45.
2 Lu Z P & Liu C T, *Acta Mater*, 50 (2002) 3501.
3 Yusub S, Baskaran G S, Krishna S B M, Rajyasree C, Babu A R & Rao D K, *Indian J Pure Appl Phys*, 49 (2011) 315.
4 Clement W, Wilnes R H & Duwez P, *Nature*, 187 (1960) 869.
5 Carter J, Fu E G, Martin M, Xie G, Zhang X, Wang Y Q, Wijesundera D, Wang X M, Chu W K, McDeavitt S M & Shao L, *Nucl Instrum Methods Phys Res B*, 267 (2009) 2827.
6 Iqbal M, Akhter J I, Hu Z Q, Zhang H F, Qayyum A & Sun W S, *J Non-Cryst Solids*, 353 (2007) 2452.
7 Raghavan R, Boopathy K, Ghisleni R, Pouchon M A, Ramamurty U & Michlera J, *Scr Mater*, 62 (2010) 462.
8 Mathur S, Vyas R, Kulriya P K, Asokan K, Sachdev K & Sharma S K, *J Alloys Compd*, 503 (2010) 192.
9 Perez-Berguist A G, Bei H, Leonard K J, Zhang Y & Zinkle S J, *Intermet*, 53 (2014) 62.
10 Menéndez E, Hynowska A, Fornell J, Suriñach S, Montserrat J, Temst K, Vantomme A, Baró M D, García-Lecina E, Pellicer E & Sort J, *J Alloys Compd*, 610 (2014) 118.
11 Cohen M H & Turnbull D, *J Chem Phys*, 31 (1959) 1164.
12 Spaepen F, *Acta Metall*, 25 (1977) 407.
13 Tang L, Peng K, Wu Y & Zhang W, *J Alloys Compd*, 695 (2017) 2136.
14 Wu Y, Peng K, Tang L & Zhang W, *Intermet*, 91 (2017) 65.
15 Brett C M A & Brett A M O, *Electrochemistry: Principles, methods and applications*, (Oxford University Press: Oxford), (1993) 456.
16 Koga G Y, Nogueira R P, Roche V, Yavari A R, Melle A K, Gallego J, Bolfarini C, Kiminami C S & Botta W J, *Surf Coat Technol*, 254 (2014) 238.
17 Kiminami C S, Souza C A C, Bonavina L F, Lima L R P A, Suriñach S, Baró M D, Bolfarini C & Botta W J, *J Non-Cryst Solids*, 356 (2010) 2651.